

Manganese–Chromium–Cyanide Clusters: Molecular $\text{MnCr}_6(\text{CN})_{18}$ and $\text{Mn}_3\text{Cr}_6(\text{CN})_{18}$ Species and a Related $\text{MnCr}_3(\text{CN})_9$ Chain Compound

Julie L. Heinrich, Jennifer J. Sokol, Allan G. Hee, and Jeffrey R. Long¹

Department of Chemistry, University of California—Berkeley, Berkeley, California 94720-1460

E-mail: jlong@cchem.berkeley.edu

Received March 20, 2001; accepted March 21, 2001

IN DEDICATION TO THE LATE PROFESSOR OLIVIER KAHN FOR HIS PIONEERING CONTRIBUTIONS TO THE FIELD OF MOLECULAR MAGNETISM

As part of an ongoing effort to design new single-molecule magnets, we are exploring synthetic routes to high-nuclearity metal–cyanide clusters. Here, we report the results of solution assembly reactions between $[(\text{Me}_3\text{tacn})\text{Cr}(\text{CN})_3]$ ($\text{Me}_3\text{tacn} = N, N', N''$ -trimethyl-1,4,7-triazacyclononane) and selected manganese(II) salts. Reaction with the perchlorate salt in the presence of $A\text{ClO}_4$ ($A = \text{Na}, \text{K}$) gives $A[(\text{Me}_3\text{tacn})_6\text{MnCr}_6(\text{CN})_{18}](\text{ClO}_4)_3$, featuring a heptanuclear cluster in which six $[(\text{Me}_3\text{tacn})\text{Cr}(\text{CN})_3]$ units surround a central Mn^{II} ion. The Mn coordination geometry closely approaches a trigonal prism, with triangular faces twisted away from a fully eclipsed position by an angle of 12.8° and 11.3° for $A = \text{Na}$ and K , respectively. The magnetic behavior of both compounds indicates weak antiferromagnetic coupling between neighboring Mn^{II} and Cr^{III} centers ($J = -3.0$ and -3.1 cm^{-1} , respectively) to give an $S = \frac{13}{2}$ ground state. Alternatively, addition of sodium tetraphenylborate to the reaction solution yields $[(\text{Me}_3\text{tacn})_6(\text{H}_2\text{O})_6\text{Mn}_3\text{Cr}_6(\text{CN})_{18}](\text{BPh}_4)_6 \cdot 12\text{H}_2\text{O}$, in which attachment of two Mn^{II} ions to the preceding cluster generates a new species with two trigonal bipyramids sharing a common vertex. This compound displays magnetic behavior consistent with weak antiferromagnetic coupling and an $S = \frac{3}{2}$ ground state. Finally, a reaction employing manganese(II) triflate is found to produce the one-dimensional solid $[(\text{Me}_3\text{tacn})_3\text{MnCr}_3(\text{CN})_9](\text{CF}_3\text{SO}_3)_2$, exhibiting a closely related chain structure, and, again, weak antiferromagnetic coupling. © 2001 Academic Press

Key Words: manganese; chromium; cyanide; cluster; chain compound; magnetic properties.

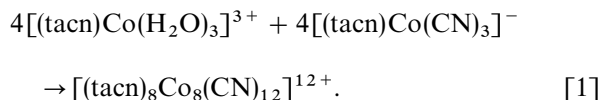
INTRODUCTION

Recently, certain metal–oxo clusters were discovered to exhibit slow magnetic relaxation at temperatures below 3 K (1–9). These species, designated single-molecule magnets, possess an energy barrier for magnetic moment reversal that arises from a ground state with a combination of high spin,

S , and axial magnetic anisotropy, $D < 0$. In order to explore the possibility of utilizing such molecules as data storage media, new clusters displaying larger values of S and $|D|$ —and, hence, higher magnetic moment reversal barriers—are sought.

Metal–cyanide cluster systems (10–23) offer several advantages over metal–oxo systems in attempting to control S and D . The preference of cyanide for spanning two transition metals in a linear bridging geometry allows a more directed approach to cluster synthesis. Further, the nature of the pairwise magnetic exchange interaction between octahedrally coordinated metal centers in such a situation is readily predicted (24, 25). Indeed, an understanding of the factors influencing the strength of that exchange interaction has enabled the synthesis of Prussian-blue-type solids with bulk magnetic ordering temperatures above room temperature (26–30). Finally, the anticipated ability to substitute a range of different metals into a given metal–cyanide cluster geometry should provide a means for adjusting both S and D in the ground state.

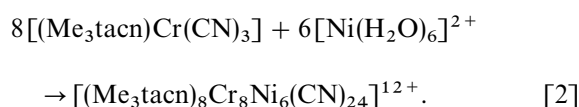
We are therefore developing methods for synthesizing high-nuclearity metal–cyanide clusters (31–33). Our approach employs assembly reactions that parallel the preparations of Prussian-blue-type solids (34, 35), but utilizes blocking ligands to inhibit growth of an extended solid structure. For example, the use of triazacyclononane (tacn) as a capping group has been shown to direct the formation of a cubic $[(\text{tacn})_8\text{Co}_8(\text{CN})_{12}]^{12+}$ cluster, representing a fundamental cage unit from the Prussian-blue-type framework (31):



Analogous clusters featuring cyclopentadienyl and carbonyl ligands have also been reported (36, 37), and other researchers have employed a similar strategy in synthesizing

¹ To whom correspondence should be addressed.

smaller, exchange-coupled metal–cyanide clusters (38–41). However, larger cluster geometries in which more than eight metal centers can be magnetically coupled are needed to achieve the exceptionally large spin states (42–44) ultimately desired in a single-molecule magnet. A simple idea for generating higher-nuclearity species involves the use of a blocking ligand on only one of the components in reaction [1], thereby permitting cluster growth to propagate further. Accordingly, the following reaction ($\text{Me}_3\text{tacn} = N,N',N''$ -trimethyl-1,4,7-triazacyclononane) in aqueous solution was found to produce a 14-metal cluster with a face-centered cubic geometry (32):



Herein, we report the results of analogous assembly reactions in which manganese(II) is used in place of nickel(II).

EXPERIMENTAL SECTION

Preparation of compounds. The compounds $[(\text{Me}_3\text{tacn})\text{Cr}(\text{CN})_3]$ and $\text{Mn}(\text{CF}_3\text{SO}_3)_2 \cdot \text{MeCN}$ were synthesized as described previously (31,45). Water was distilled and deionized with a Milli-Q filtering system. All other reagents were obtained from commercial vendors and used without further purification.

$\text{Na}[(\text{Me}_3\text{tacn})_6\text{MnCr}_6(\text{CN})_{18}](\text{ClO}_4)_3$ (**1**). Solid portions of $\text{Mn}(\text{ClO}_4)_2 \cdot 6\text{H}_2\text{O}$ (0.13 g, 0.35 mmol) and NaClO_4 (0.020 g, 0.16 mmol) were added to a stirred solution of $[(\text{Me}_3\text{tacn})\text{Cr}(\text{CN})_3]$ (0.13 g, 0.45 mmol) in 5 mL of water. The addition of 50 mL of methanol to the resulting yellow solution induced precipitation of a yellow solid, which was collected by filtration and dried in air to give 0.14 g (86%) of product. Single crystals in the form of yellow hexagonal plates were obtained by slow evaporation of the aqueous solution. Absorption spectrum (H_2O): λ_{max} (ϵ_{M}) 339 (370), 361 (sh, 180), 425 (300) nm. IR (KBr): ν_{CN} 2149 cm^{-1} . Anal. Calcd for $\text{C}_{72}\text{H}_{126}\text{Cl}_3\text{Cr}_6\text{MnN}_{36}\text{NaO}_{12}$: C, 39.48; H, 5.89; N, 23.02. Found: C, 39.79; H, 6.05; N, 22.93.

$\text{K}[(\text{Me}_3\text{tacn})_6\text{MnCr}_6(\text{CN})_{18}](\text{ClO}_4)_3$ (**2**). This compound was prepared by a procedure analogous to that described for the preparation of **1**. IR (KBr): ν_{CN} 2149 cm^{-1} . Anal. Calcd for $\text{C}_{72}\text{H}_{126}\text{Cl}_3\text{Cr}_6\text{KMnN}_{36}\text{O}_{12}$: C, 39.30; H, 5.77; N, 22.92. Found: C, 39.43; H, 6.04; N, 22.80.

$[(\text{Me}_3\text{tacn})_6(\text{H}_2\text{O})_6\text{Mn}_3\text{Cr}_6(\text{CN})_{18}](\text{BPh}_4)_6 \cdot 12\text{H}_2\text{O}$ (**3**). Solid $\text{Mn}(\text{ClO}_4)_2 \cdot 6\text{H}_2\text{O}$ (0.030 g, 0.083 mmol) was added to a solution of $[(\text{Me}_3\text{tacn})\text{Cr}(\text{CN})_3]$ (0.050 g, 0.17 mmol) in 10 mL of water. The resulting yellow solution was heated to 80°C, and a solution of NaBPh_4 (0.065 g, 0.19 mmol) in 5 mL of water was added dropwise. The solution was con-

centrated to a volume of approx. 10 mL, and allowed to cool to give yellow needle-shaped crystals. The crystals were collected by filtration, and dissolved in 10 mL of a 1:1 (volume: volume) mixture of acetone and water. Evaporation of the acetone produced yellow block-shaped crystals of $\mathbf{3} \cdot 12\text{H}_2\text{O}$ suitable for X-ray analysis; these were collected by filtration and dried in air to yield 0.11 g (95%) of product. Absorption spectrum (DMF): λ_{max} (ϵ_{M}) 346 (490), 436 (290) nm. IR (KBr): ν_{CN} 2165, 2115, 2097 cm^{-1} . Anal. Calcd for $\text{C}_{216}\text{H}_{270}\text{B}_6\text{Cr}_6\text{MnN}_{36}\text{O}_{18}$: C, 61.59; H, 6.75; N, 11.97. Found: C, 61.66; H, 6.80; N, 11.77. The water content of this compound was confirmed by thermogravimetric analysis.

$[(\text{Me}_3\text{tacn})_3\text{MnCr}_3(\text{CN})_9](\text{CF}_3\text{SO}_3)_2$ (**4**). Solid $\text{Mn}(\text{CF}_3\text{SO}_3)_2 \cdot \text{MeCN}$ (0.070 g, 0.18 mmol) was added to a solution of $[(\text{Me}_3\text{tacn})\text{Cr}(\text{CN})_3]$ (0.035 g, 0.12 mmol) in 7 mL of methanol. Diffusing ether into the resulting yellow solution produced yellow block-shaped crystals suitable for X-ray analysis; these were collected by filtration and dried in air to yield 0.036 g (74%) of product. IR (KBr): ν_{CN} 2164, 2124 cm^{-1} . Anal. Calcd for $\text{C}_{38}\text{H}_{63}\text{Cr}_3\text{F}_6\text{MnN}_{18}\text{O}_6\text{S}_2$: C, 36.31; H, 5.05; N, 20.06. Found: C, 36.10; H, 4.99; N, 19.29.

X-ray structure determinations. Structures were determined for the compounds listed in Table 1. Single crystals were coated with Paratone-N oil, attached to glass fibers, transferred to a Siemens SMART diffractometer, and cooled in a dinitrogen stream. Initial lattice parameters were obtained from a least-squares analysis of more than 30 centered reflections; these parameters were later refined against all data. None of the crystals showed significant decay during data collection. Data were integrated and corrected for Lorentz and polarization effects using SAINT, and were corrected for absorption effects using SADABS. Space group assignments were based on systematic absences, E statistics, and successful refinement of the structures. Structures were solved by direct methods with the aid of successive difference Fourier maps, and refined against all data using the SHELXTL 5.0 software package. Thermal parameters for all nonhydrogen atoms except those exhibiting disorder were refined anisotropically. Hydrogen atoms associated with water molecules and disordered methylene carbon atoms were not included in the structural refinements. All other hydrogen atoms were assigned to ideal positions and refined using a riding model with an isotropic thermal parameter 1.2 times that of the attached carbon atom (1.5 times for methyl hydrogens). The oxygen atoms of the perchlorate anions in the structures of **1** and **2** are all heavily disordered, and were assigned to multiple partially occupied positions. One of the solvate water molecules in the structure of $\mathbf{3} \cdot 12\text{H}_2\text{O}$ is disordered over two positions. Methylene carbon atoms in the structure of **4** were modeled as being disordered over two equally occupied positions, corresponding to two distinct Me_3tacn ligand conformations. Crystallographic data (excluding structure factors) for

TABLE 1
Crystallographic Data^a for Na[(Me₃tacn)₆MnCr₆(CN)₁₈](ClO₄)₃ (1), K[(Me₃tacn)₆MnCr₆(CN)₁₈](ClO₄)₃ (2), [(Me₃tacn)₆(H₂O)₆Mn₃Cr₆(CN)₁₈](BPh₄)₆ · 24H₂O (3 · 12H₂O), and [(Me₃tacn)₃MnCr₃(CN)₉](CF₃SO₃)₂ (4)

	1	2	3 · 12H ₂ O	4
Formula	C ₇₂ H ₁₂₆ Cl ₃ Cr ₆ MnN ₃₆ NaO ₁₂	C ₇₂ H ₁₂₆ Cl ₃ Cr ₆ KMnN ₃₆ O ₁₂	C ₂₁₆ H ₂₉₄ B ₆ Cr ₆ MnN ₃₆ O ₃₀	C ₃₈ H ₆₃ Cr ₃ F ₆ MnN ₁₈ O ₆ S ₂
Formula wt	2184.37	2200.48	4368.17	1257.12
<i>T</i> (K)	179	147	160	163
Space group	<i>P</i> $\bar{3}$ 1 <i>c</i>	<i>P</i> $\bar{3}$ 1 <i>c</i>	<i>R</i> $\bar{3}$	<i>P</i> 6 ₃ / <i>m</i>
<i>Z</i>	2	2	3	2
<i>a</i> (Å)	14.1437(1)	14.1571(2)	27.3488(3)	15.3315(1)
<i>c</i> (Å)	27.7900(2)	27.8652(2)	26.2300(6)	13.6233(3)
<i>V</i> (Å ³)	4814.43(6)	4836.6(1)	16990.5(5)	2773.21(7)
<i>d</i> _{calc} (g/cm ³)	1.507	1.511	1.281	1.505
<i>R</i> ₁ (w <i>R</i> ₂) ^b (%)	3.57 (8.51)	4.08 (9.55)	5.79 (11.70)	5.78 (14.06)

^a Obtained with graphite monochromated MoK α ($\lambda = 0.71073$ Å) radiation.

^b $R_1 = \sum ||F_o| - |F_c|| / \sum |F_o|$, $wR_2 = \{\sum [w(F_o^2 - F_c^2)^2] / \sum [w(F_o^2)]\}^{1/2}$.

all four structures have been deposited with the Cambridge Crystallographic Data Centre as supplementary publications CCDC-151692 to -151695. Copies of the data can be obtained free of charge on application to CCDC, 12 Union Road, Cambridge CB2 1EC, UK (fax: +(44)1223-336-033; e-mail: deposit@ccdc.cam.ac.uk).

Magnetic susceptibility measurements. DC magnetic susceptibility data were collected using a Quantum Design MPMS2 SQUID magnetometer. Data were corrected for diamagnetic contributions using Pascal's constants. A temperature-independent paramagnetism of approx. 200×10^{-6} cgsu per metal center was assumed for each compound. The data were fit to theoretical models using a relative error minimization routine (MAGFIT 3.1) (46), except in the case of compound 3, where magnetic data were simulated using MAGPACK (47). All reported coupling constants are based on exchange Hamiltonians of the form $\hat{H} = -2J\hat{S}_i \cdot \hat{S}_j$.

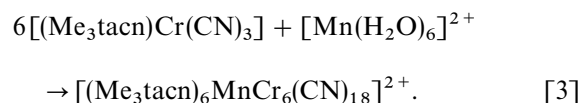
Other physical measurements. Absorption spectra were measured with a Hewlett–Packard 8453 spectrophotometer. Infrared spectra were recorded on a Mattson Infinity System FTIR spectrometer or on a Nicolet Avatar 360 FTIR spectrometer equipped with an attenuated total reflectance accessory. Thermogravimetric analyses were carried out in a dinitrogen atmosphere with a TA Instruments TGA 2950.

RESULTS AND DISCUSSION

Syntheses

The product isolated from the reaction between [(Me₃tacn)Cr(CN)₃] and [Mn(H₂O)₆]²⁺ depends somewhat on the choice of counteranion. With perchlorate, a compound of formula [(Me₃tacn)₆MnCr₆(CN)₁₈](ClO₄)₂ · 2H₂O containing a heptanuclear cluster is obtained, despite the presence of an excess of the manga-

nese(II) salt:



Single crystals of this compound suitable for X-ray analysis, however, could not be grown without addition of sodium or potassium perchlorate, leading to formation of Na[(Me₃tacn)₆MnCr₆(CN)₁₈](ClO₄)₃ (1) and K[(Me₃tacn)₆MnCr₆(CN)₁₈](ClO₄)₃ (2). Alternatively, addition of sodium tetraphenylborate to the reaction solution gives [(Me₃tacn)₆(H₂O)₆Mn₃Cr₆(CN)₁₈](BPh₄)₆ · 12H₂O (3), featuring a nine-metal cluster. The analogous reaction carried out with manganese(II) triflate in methanol instead generates the one-dimensional solid [(Me₃tacn)₃MnCr₃(CN)₉](CF₃SO₃)₂ (4). A similar counteranion dependence is encountered in reaction [2], where an [(Me₃tacn)₈Cr₈Ni₅(CN)₂₄]¹⁰⁺ cluster with an open cage geometry is obtained when nickel(II) iodide is used in place of nickel(II) perchlorate (33).

Trigonal Prismatic MnCr₆(CN)₁₈ Cluster

As shown in Fig. 1, the crystal structure of Na[(Me₃tacn)₆MnCr₆(CN)₁₈](ClO₄)₃ (1) reveals a [(Me₃tacn)₆MnCr₆(CN)₁₈]²⁺ cluster consisting of a central Mn^{II} ion surrounded by six [(Me₃tacn)Cr(CN)₃] complexes. Surprisingly, the coordination of the Mn center by the nitrogen ends of six cyanide ligands approximates a trigonal prismatic geometry, with rigorously parallel triangular faces twisted about the threefold axis in an angle $\phi = 12.8^\circ$ away from a fully eclipsed position. Selected geometric parameters for the cluster are listed in Table 2. Note that the bridging cyanide ligands deviate significantly from the usual linear geometry, with an Mn–N–C angle of $152.7(2)^\circ$.

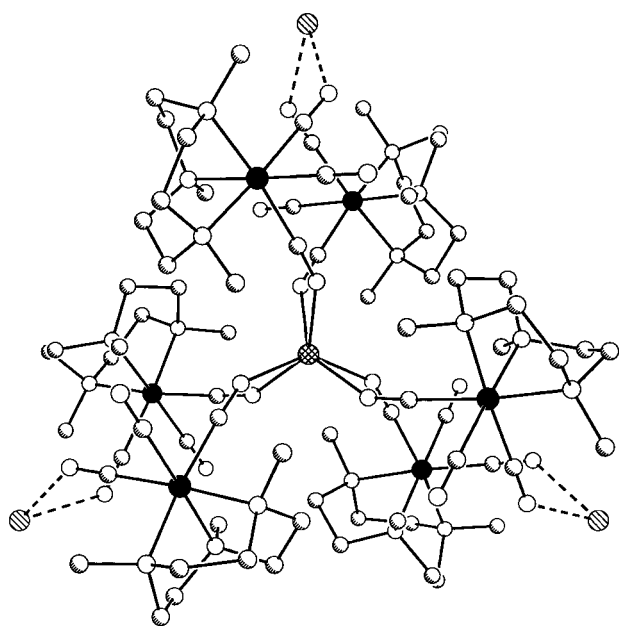


FIG. 1. Structure of the trigonal prismatic $[\text{MnCr}_6(\text{CN})_{18}(\text{Me}_3\text{tacn})_6]^{2+}$ cluster in compound **1**. Black, cross-hatched, shaded, white, and hatched spheres represent Cr, Mn, C, N, and Na atoms, respectively; H atoms are omitted for clarity. The cluster exhibits crystallographically imposed D_3 symmetry, with the Mn atom positioned on the three-fold rotation axis.

Similarly bent cyanide bridges have been observed previously in the nonmolecular solids $[\text{Mn}(\text{en})_3][\text{Cr}(\text{CN})_6]_2 \cdot 4\text{H}_2\text{O}$ and $[\text{Mn}(\text{bispicen})_3][\text{Cr}(\text{CN})_6]_2 \cdot 6.5\text{H}_2\text{O} \cdot 0.5\text{EtOH}$ (bispicen = *N,N'*-bis(2-pyridylmethyl)-1,2-ethanediamine), which feature a $\text{Cr}^{\text{III}}\text{-C-N-Mn}^{\text{II}}$ connectivity with Mn-N-C angles falling in the ranges $145.7(3)^\circ$ – $167.4(3)^\circ$ and $147.1(6)^\circ$ – $177.7(6)^\circ$, respectively (48, 49). Although the Mn centers in these solids exhibit a distorted octahedral coordination geometry, in both cases, the bent bridging arrangement is associated with a peak in the infrared spectrum close to the $\nu_{\text{CN}} = 2149\text{ cm}^{-1}$ band observed for compound **1**. This is slightly lower in energy than the $\nu_{\text{CN}} = 2170\text{ cm}^{-1}$ band corresponding to the presumably more linear cyanide bridges in the Prussian blue analogue $\text{CsMn}[\text{Cr}(\text{CN})_6] \cdot \text{H}_2\text{O}$ (50). Replacing the Na^+ ions with K^+ ions generates the isostructural compound $\text{K}[(\text{Me}_3\text{tacn})_6\text{MnCr}_6(\text{CN})_{18}](\text{ClO}_4)_3$ (**2**), featuring a slightly smaller twist angle of $\phi = 11.3^\circ$ away from an ideal trigonal prismatic coordination of the Mn center.

Transition-metal complexes adopting a trigonal prismatic coordination geometry are now well established (51–54), and a number of examples involving high-spin Mn^{II} centers have been structurally characterized (55–60). The preference for trigonal prismatic coordination over the octahedral coordination favored by ligand–ligand repulsion has been variously attributed to interactions between ligand donor atoms, molecular orbital stabilization, chelating

ligand constraints, and crystal packing forces (61–64). For high-spin Mn^{II} complexes, in which neither geometry is favored by a ligand-field stabilization energy (55, 63), the latter two factors are of chief importance. While the Mn^{II} centers in compounds **1** and **2** are coordinated by only monodentate $[(\text{Me}_3\text{tacn})\text{Cr}(\text{CN})_3]$ ligands, we propose that interactions between the terminal cyanide groups of these complex ligands and alkali metal cations (see Fig. 1) help stabilize the trigonal prismatic geometry. The interactions lead to large pseudochelate rings of connectivity $-\text{NC-Cr-CN} \cdots \text{A} \cdots \text{NC-Cr-CN}-$, which combine with an efficient means of packing the rigid $[(\text{Me}_3\text{tacn})\text{Cr}(\text{CN})_3]$ ligands to prescribe the Mn coordination geometry. Each alkali metal cation interacts with pairs of cyanide ligands from three different clusters, resulting in a coordination geometry that is intermediate between trigonal prismatic and octahedral (with twist angles of $\phi = 28.8^\circ$ and 31.7° in the structures of **1** and **2**, respectively). Figure 2 depicts a portion of the ensuing two-dimensional hexagonal net from the structure of **1**, in which perchlorate anions occupy the hexagonal openings. Although high-quality crystals of $[(\text{Me}_3\text{tacn})_6\text{MnCr}_6(\text{CN})_{18}](\text{ClO}_4)_2$ have not yet been obtained, we expect an octahedral coordination geometry for the Mn center in the absence of the alkali metal cations required to form this stable two-dimensional lattice.

Magnetic susceptibility data were measured for compounds **1** and **2** over the temperature range 2–295 K.

TABLE 2
Selected Mean Interatomic Distances (Å) and Angles ($^\circ$) for $\text{Na}[(\text{Me}_3\text{tacn})_6\text{MnCr}_6(\text{CN})_{18}](\text{ClO}_4)_3$ (**1**), $\text{K}[(\text{Me}_3\text{tacn})_6\text{MnCr}_6(\text{CN})_{18}](\text{ClO}_4)_3$ (**2**), $[(\text{Me}_3\text{tacn})_6(\text{H}_2\text{O})_6\text{Mn}_3\text{Cr}_6(\text{CN})_{18}](\text{BPh}_4)_6 \cdot 24\text{H}_2\text{O}$ (**3** · $12\text{H}_2\text{O}$), and $[(\text{Me}_3\text{tacn})_3\text{MnCr}_3(\text{CN})_9](\text{CF}_3\text{SO}_3)_2$ (**4**)

	1	2	3 · 12H ₂ O	4
Cr–C	2.071(7)	2.069(9)	2.055(4)	2.056(8)
Mn–N	2.272	2.272	2.221(4)	2.207
C–N ^a	1.148(5)	1.148(4)	1.151(6)	1.15(1)
Cr–N	2.110(4)	2.110(4)	2.105(4)	2.100(6)
Mn–O			2.164(5)	
A–N ^b	2.519	2.642		
C–Cr–C	89.3(9)	89(2)	88.3(6)	89(1)
Cr–C–N	177(2)	176.5(8)	176(1)	176(1)
N–Mn–N	79.9 ^c 83.8 ^d	80.3 ^c 83.4 ^d	90.2(8)	90.0(8)
Mn–N–C	152.7	153.4	173.4 ^e 167.2 ^f	164.7
C–Cr–N	94(1)	94(2)	94.0(9)	94(1)
N–Cr–N	83.4(4)	83.5(3)	83.6(2)	83.5(3)

^a Within a cyanide ligand.

^b A = Na, K.

^c N atoms are located on a rectangular edge.

^d N atoms are located on a triangular edge.

^e Angles involve the central Mn atom.

^f Angles involve the outer Mn atoms.

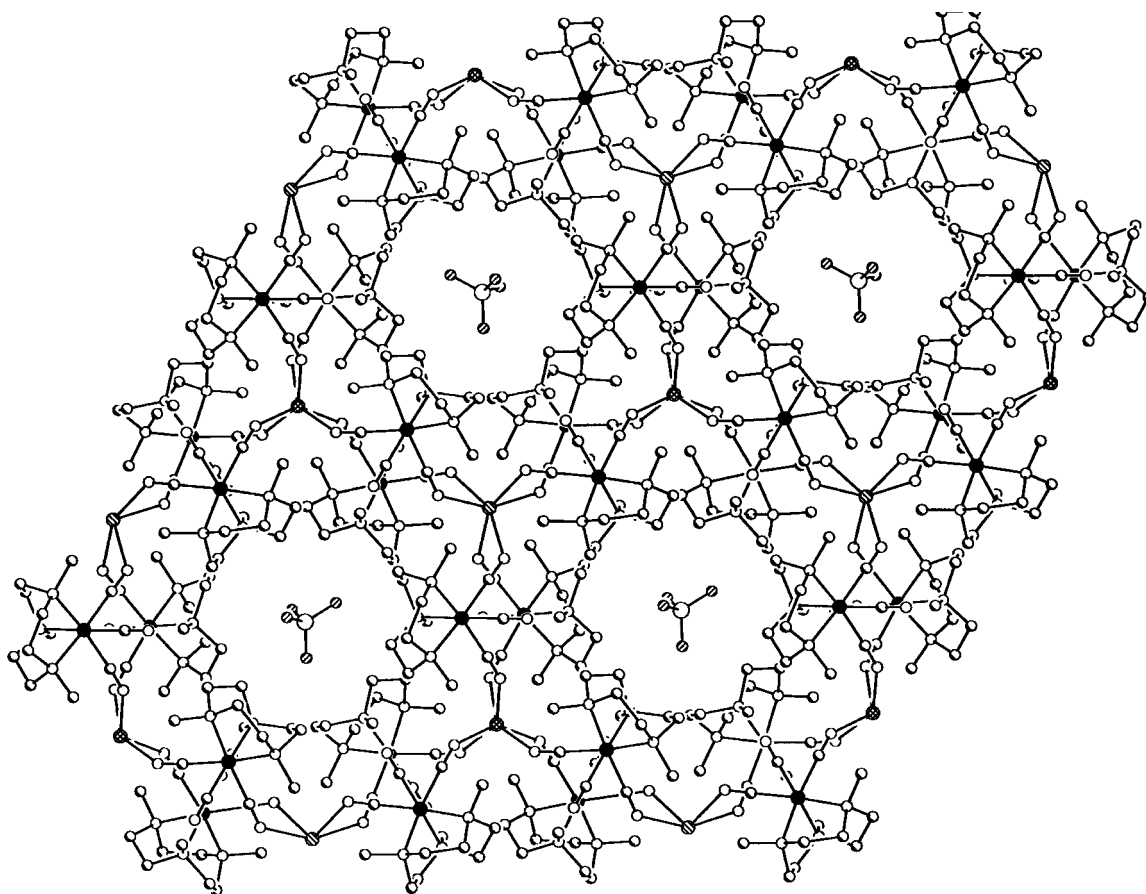


FIG. 2. A portion of a two-dimensional sheet in the structure of $\text{Na}[(\text{Me}_3\text{tacn})_6\text{MnCr}_6(\text{CN})_{18}](\text{ClO}_4)_3$ (**1**). Black, cross-hatched, shaded, small white, top left to bottom right hatched, large white, and top right to bottom left hatched spheres represent Cr, Mn, C, N, Na, Cl, and O atoms, respectively; H atoms are omitted for clarity. Only one arrangement of the oxygen atoms is depicted for the severely disordered perchlorate anions.

Measurements were carried out at a field strength of only 100 G, owing to the anticipated weakness of the magnetic exchange interactions. The results for compound **2** are displayed in Fig. 3. At 295 K, $\chi^{\text{M}}T$ is $14.6 \text{ cm}^3\text{K/mol}$, just below the value of $15.625 \text{ cm}^3\text{K/mol}$ expected for one Mn^{II} ($S = \frac{5}{2}$) ion and six Cr^{III} ($S = \frac{3}{2}$) ions in the absence of any exchange coupling. As the temperature is lowered, $\chi^{\text{M}}T$ drops, reaching a minimum at approx. 50 K before rising steeply. This behavior is consistent with weak antiferromagnetic coupling between Mn and Cr to give an $S = \frac{13}{2}$ ground state. The fact that $\chi^{\text{M}}T$ extends to values above the expected maximum of $24.375 \text{ cm}^3\text{K/mol}$ at very low temperatures likely indicates the presence of some slight ferromagnetic coupling between molecules. Since all six Cr atoms in the $[(\text{Me}_3\text{tacn})_6\text{MnCr}_6(\text{CN})_{18}]^{2+}$ cluster are equivalent by symmetry, the data were fitted to the Van Vleck equation using a single pairwise exchange parameter and an exchange Hamiltonian of the form

$$\hat{H} = -2J[\hat{S}_{\text{Mn}} \cdot (\hat{S}_{\text{Cr}(1)} + \hat{S}_{\text{Cr}(2)} + \hat{S}_{\text{Cr}(3)} + \hat{S}_{\text{Cr}(4)} + \hat{S}_{\text{Cr}(5)} + \hat{S}_{\text{Cr}(6)})]. \quad [4]$$

The best fit to the data (see Fig. 3) was obtained with a coupling constant of $J = -3.1 \text{ cm}^{-1}$ and $g = 2.01$. This is slightly weaker than the coupling constant of $J = -4.0 \text{ cm}^{-1}$ observed in the heptanuclear cluster $[\text{Cr}(\text{CNMn}(\text{TrispicMeen}))_6]^{9+}$ (TrispicMeen = *N,N,N'*-(tris(2-pyridylmethyl)-*N'*-methylethane)-1,2-diamine) with analogous $\text{Cr}^{\text{III}}\text{-CN-Mn}^{\text{II}}$ exchange pathways (65). Unfortunately, a crystal structure of the foregoing species is not available for comparison; however, the infrared absorption band at $\nu_{\text{CN}} = 2150 \text{ cm}^{-1}$ (65) suggests that it too contains bent cyanide bridges. Magnetic susceptibility data for compound **1** were nearly identical to the data obtained for compound **2**, and were best fit with $J = -3.0 \text{ cm}^{-1}$ and $g = 1.95$.

$\text{Mn}_3\text{Cr}_6(\text{CN})_{18}$ Cluster

Despite having a labile central Mn^{II} ion, the preceding $[(\text{Me}_3\text{tacn})_6\text{MnCr}_6(\text{CN})_{18}]^{2+}$ cluster is suggestive of a platform to which additional magnetically coupled metal ions could perhaps be attached. Indeed, one such construct is evident in the crystal structure of $[(\text{Me}_3\text{tacn})_6(\text{H}_2\text{O})_6]$

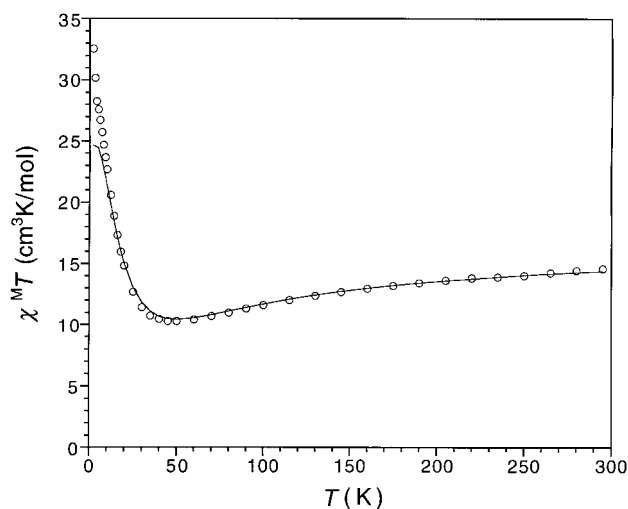


FIG. 3. Magnetic behavior of $\text{K}[(\text{Me}_3\text{tacn})_6\text{MnCr}_6(\text{CN})_{18}](\text{ClO}_4)_3$ (**2**), as measured in an applied field of 100 G. The solid line represents the calculated fit to the data with $J = -3.1 \text{ cm}^{-1}$ and $g = 2.01$.

$\text{Mn}_3\text{Cr}_6(\text{CN})_{18}](\text{BPh}_4)_6 \cdot 24\text{H}_2\text{O}$ (**3**·12 H_2O). Here, six of the terminal cyanide ligands coordinate two added $[\text{Mn}(\text{H}_2\text{O})_3]^{2+}$ moieties, giving rise to the $[(\text{Me}_3\text{tacn})_6(\text{H}_2\text{O})_6\text{Mn}_3\text{Cr}_6(\text{CN})_{18}]^{6+}$ cluster displayed in Fig. 4. The metal–cyanide framework of this S_6 -symmetry cluster consists of two trigonal bipyramids sharing a common axial

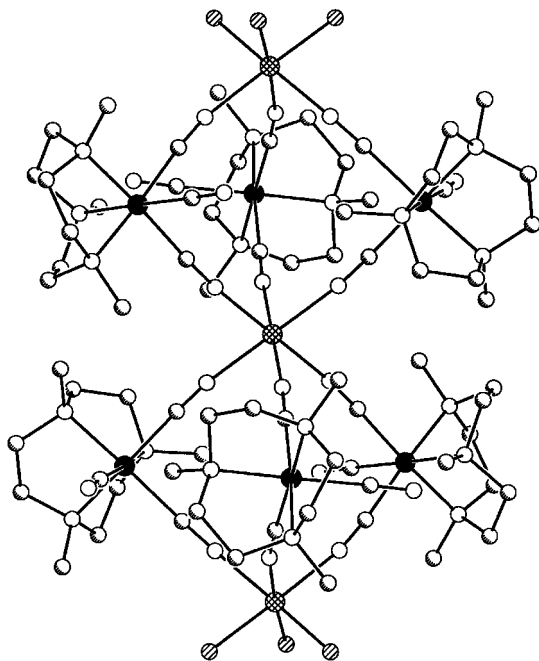


FIG. 4. Structure of the $[(\text{H}_2\text{O})_6\text{Mn}_3\text{Cr}_6(\text{CN})_{18}(\text{Me}_3\text{tacn})_6]^{6+}$ cluster in **3**·12 H_2O . Black, cross-hatched, shaded, white, and hatched spheres represent Cr, Mn, C, N, and O atoms, respectively; H atoms are omitted for clarity. The cluster resides on a 3 symmetry site with the Mn atoms positioned on the three-fold rotation axis.

vertex. Two significant differences are apparent in comparing its geometry to that of the trigonal prismatic clusters found in the structures of **1** and **2** (see Table 2): all three Mn centers exhibit octahedral coordination, and the bridging cyanide ligands adopt a significantly more linear arrangement. The latter observation is consistent with the higher energy ($\nu_{\text{CN}} = 2165 \text{ cm}^{-1}$) of the corresponding absorption band in the infrared spectrum of compound **3**. Although the remaining six terminal cyanide ligands of the cluster are probably too hindered to bind additional metal ions, we are exploring the possibility of extending its reactivity by replacing the water ligands on the outer Mn centers with cyanide ligands.

Figure 5 shows the magnetic behavior of compound **3** over the temperature range 5–280 K. At 280 K, $\chi^M T$ is $21.9 \text{ cm}^3\text{K/mol}$, slightly below the uncoupled limit of $24.375 \text{ cm}^3\text{K/mol}$ expected for six Cr^{III} ($S = \frac{3}{2}$) ions and three Mn^{II} ($S = \frac{5}{2}$) ions. As the temperature is lowered, $\chi^M T$ decreases, again indicating antiferromagnetic exchange coupling between the Mn^{II} and Cr^{III} centers. The greater number of Mn^{II} centers, however, reduces the total spin of the ground state to $S = \frac{3}{2}$, such that $\chi^M T$ continues to decrease, reaching a value of $2.85 \text{ cm}^3\text{K/mol}$ at 5 K (not quite achieving the predicted value of $1.875 \text{ cm}^3\text{K/mol}$). The arrangement of the spin interactions in the $[(\text{Me}_3\text{tacn})_6(\text{H}_2\text{O})_6\text{Mn}_3\text{Cr}_6(\text{CN})_{18}]^{6+}$ cluster is one that is not amenable to analysis using the vector-coupling procedure of Kambe (66). Attempts at simulating the data therefore required use of the irreducible tensor operator technique (47), a computationally intensive process. Two distinct types of magnetic exchange pathways are present in the cluster: one across cyanide bridges connecting a Cr^{III} ion to the central Mn^{II} ion, and the other across the slightly more bent

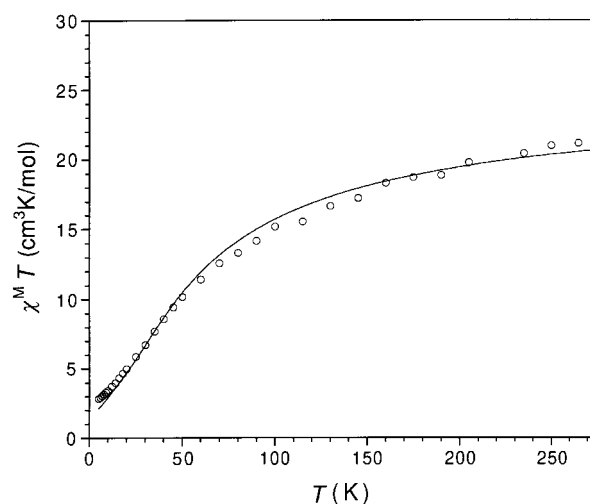


FIG. 5. Magnetic behavior of $[(\text{Me}_3\text{tacn})_6(\text{H}_2\text{O})_6\text{Mn}_3\text{Cr}_6(\text{CN})_{18}]$ (BPh_4) $_6 \cdot 12\text{H}_2\text{O}$ (**3**), as measured in an applied field of 200 G. The solid line represents a rough simulation of the data assuming $J = -3.0 \text{ cm}^{-1}$ and $g = 2.00$.

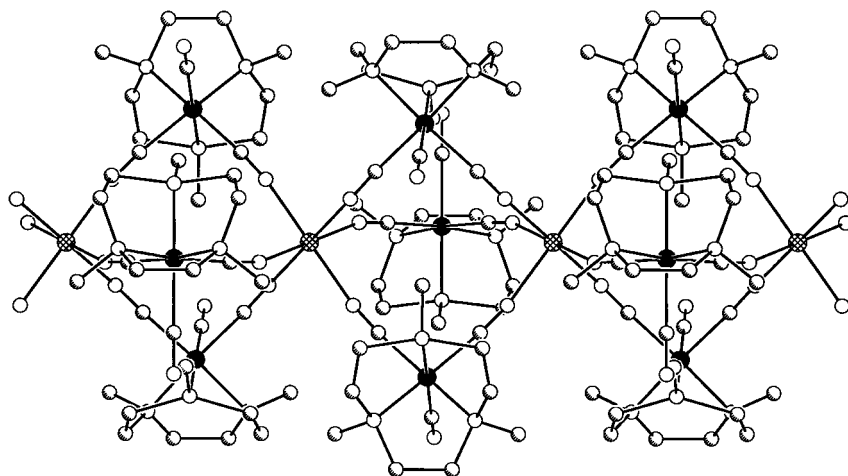


FIG. 6. A portion of the one-dimensional $[\text{MnCr}_3(\text{CN})_9(\text{Me}_3\text{tacn})_3]^{2+}$ chain in the structure of compound **4**. Black, cross-hatched, shaded, and white spheres represent Cr, Mn, C, and N atoms, respectively; H atoms are omitted for clarity. The chain runs along a 6_3 screw axis.

cyanide bridges connecting a Cr^{III} ion to an outer Mn^{II} ion. Assuming the two pathways to be equivalent, a rough simulation of the data (see Fig. 5) was obtained using an exchange Hamiltonian of the following form with $J = -3.0 \text{ cm}^{-1}$ and $g = 2.00$:

$$\hat{H} = -2J[(\hat{S}_{\text{Mn}(1)} + \hat{S}_{\text{Mn}(2)}) \cdot (\hat{S}_{\text{Cr}(1)} + \hat{S}_{\text{Cr}(2)} + \hat{S}_{\text{Cr}(3)}) + (\hat{S}_{\text{Mn}(1)} + \hat{S}_{\text{Mn}(3)}) \cdot (\hat{S}_{\text{Cr}(4)} + \hat{S}_{\text{Cr}(5)} + \hat{S}_{\text{Cr}(6)})]. \quad [5]$$

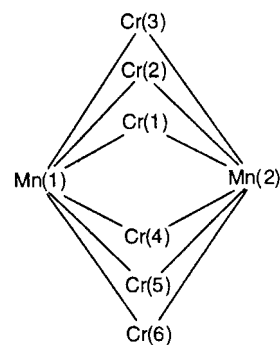
This coupling constant compares well with the J values of -2.5 and -2.7 cm^{-1} extracted from the ordering temperatures for the Prussian-blue-type ferrimagnets $\text{Mn}_3[\text{Cr}(\text{CN})_6]_2 \cdot 7.5\text{H}_2\text{O}$ (67, 68) and $\text{CsMn}[\text{Cr}(\text{CN})_6] \cdot \text{H}_2\text{O}$ (50, 69), respectively. The more linear cyanide bridges in these compounds might be expected to result in a magnetic exchange interaction significantly stronger than that observed with the bent cyanide bridges discussed above. We note, however, that the increase in σ and π overlap between orbitals on the N and Mn atoms should strengthen both antiferromagnetic ($\text{Cr}(t_{2g}^3)\text{-CN-Mn}(t_{2g}^3)$) and ferromagnetic ($\text{Cr}(t_{2g}^3)\text{-CN-Mn}(e_g^2)$) components of the exchange interaction, perhaps to differing degrees.

One-Dimensional $\text{MnCr}_3(\text{CN})_9$ Chain

An extended version of the $[(\text{Me}_3\text{tacn})_6(\text{H}_2\text{O})_6\text{Mn}_3\text{Cr}_6(\text{CN})_{18}]^{6+}$ cluster structure is present in the one-dimensional compound $[(\text{Me}_3\text{tacn})_3\text{MnCr}_3(\text{CN})_9](\text{CF}_3\text{SO}_3)_2$ (**4**). As shown in Fig. 6, each Mn_2Cr_3 trigonal bipyramid now shares both of its axial Mn vertices to form an infinite chain. Interatomic distances and angles within a chain approximate those observed in the cluster of $\mathbf{3} \cdot 12\text{H}_2\text{O}$ (see Table 2). The Mn–N–C angle of $164.7(5)^\circ$ is less bent than that in the structures of **1** and **2** and marginally more bent than that in the structure of $\mathbf{3} \cdot 12\text{H}_2\text{O}$, in agreement with the position of the infrared absorption band at $\nu_{\text{CN}} = 2164 \text{ cm}^{-1}$. The

chains in **4** are arranged in a hexagonal close-packed array, with triflate counteranions situated in the intervening triangular channels.

The magnetic behavior of compound **4** over the temperature range 5–295 K is displayed in Fig. 7. At 295 K, χ^{MT} is $8.29 \text{ cm}^3\text{K/mol}$, slightly below the value of $10.00 \text{ cm}^3\text{K/mol}$ expected in the absence of exchange coupling. As the temperature is lowered, χ^{MT} varies in a manner similar to that observed for compound **2** (see Fig. 3), reaching a minimum at approx. 60 K before rising steeply. The trend is once again consistent with weak antiferromagnetic coupling between the Mn^{II} and Cr^{III} ions; however, higher values of χ^{MT} are attained at low temperature as a result of the extended chain structure. The approach typically employed in attempting to simulate the magnetic data for a one-dimensional chain is to calculate the behavior for a sequence of cyclic oligomers, increasing the size until one can extrapolate to the infinite chain (70, 71). Unfortunately, the size of the repeat unit in the bimetallic $[(\text{Me}_3\text{tacn})_3\text{MnCr}_3(\text{CN})_9]_n^{2n+}$ chains of compound **4** render this approach untenable. Only results for an initial member of the sequence, a hypothetical $[(\text{Me}_3\text{tacn})_6\text{Mn}_2\text{Cr}_6(\text{CN})_{18}]^{4+}$ ($n = 2$) species with the following spin connectivity, could be calculated:



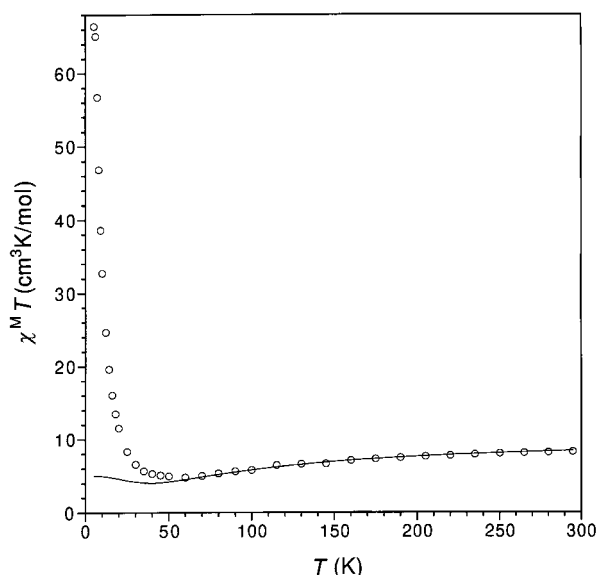


FIG. 7. Magnetic behavior of $[(\text{Me}_3\text{tacn})_3\text{MnCr}_3(\text{CN})_9](\text{CF}_3\text{SO}_3)_2$ (**4**), as measured in an applied field of 1000 G. The solid line indicates the behavior calculated for a hypothetical, cyclic $[(\text{Me}_3\text{tacn})_6\text{Mn}_2\text{Cr}_6(\text{CN})_{18}]^{4+}$ species with $J = -3.3 \text{ cm}^{-1}$ and $g = 2.00$.

A single pairwise exchange parameter between the Cr^{III} ($S = \frac{3}{2}$) and Mn^{II} ($S = \frac{5}{2}$) centers was again assumed, along with an exchange Hamiltonian of the following form.

$$\hat{H} = -2J[(\hat{S}_{\text{Mn}(1)} + \hat{S}_{\text{Mn}(2)}) \cdot (\hat{S}_{\text{Cr}(1)} + \hat{S}_{\text{Cr}(2)} + \hat{S}_{\text{Cr}(3)} + \hat{S}_{\text{Cr}(4)} + \hat{S}_{\text{Cr}(5)} + \hat{S}_{\text{Cr}(6)})]. \quad [6]$$

The solid line in Fig. 7 indicates the behavior calculated for the cyclic species with $J = -3.3 \text{ cm}^{-1}$ and $g = 2.00$. As expected, reasonable agreement with the data for compound **4** is observed at high temperatures, but at lower temperatures the value of $\chi^{\text{M}}T$ for the ferrimagnetic chain diverges.

Efforts to apply the methods exemplified here with the assembly of high-nuclearity manganese–chromium–cyanide clusters in the generation of new single-molecule magnets are ongoing. In particular, we are pursuing reactions that attempt to incorporate transition-metal ions with a more substantial zero-field splitting—intended to impart magnetic anisotropy—into these and other cluster geometries.

ACKNOWLEDGMENTS

This research was funded by the University of California, the Hellman Family Faculty Fund, the Camille and Henry Dreyfus Foundation, and NSF Grants CHE-9727410 and CHE-0072691. NSF is also gratefully acknowledged for supplying a fellowship to J.J.S. We thank Matthew P. Shores for experimental assistance, Dr. C. Crawford and Unilever for a donation of Me_3tacn , Professors D. N. Hendrickson and E. Coronado for supplying software used to simulate magnetic data, Professor J. K.

McCusker for many helpful discussions, Professors A. M. Stacy and A. Zettl for use of the SQUID magnetometers, A. Kollias and Professor W. A. Lester for use of a computer, Professor J. Arnold for use of the thermogravimetric analysis instrument, and Professor T. D. Tilley for use of the infrared spectrometer.

REFERENCES

1. R. Sessoli, H.-L. Tsai, A. R. Schake, S. Wang, J. B. Vincent, K. Folting, D. Gatteschi, G. Christou, and D. N. Hendrickson, *J. Am. Chem. Soc.* **115**, 1804 (1993).
2. R. Sessoli, D. Gatteschi, A. Caneschi, and M. A. Novak, *Nature* **365**, 141 (1993).
3. A.-L. Barra, P. Debrunner, D. Gatteschi, C. E. Schultz, and R. Sessoli, *Europhys. Lett.* **35**, 133 (1996).
4. S. M. J. Aubin, M. W. Wemple, D. M. Adams, H.-L. Tsai, G. Christou, and D. N. Hendrickson, *J. Am. Chem. Soc.* **118**, 7746 (1996).
5. S. L. Castro, Z. Sun, C. M. Grant, J. C. Bolinger, D. N. Hendrickson, and G. Christou, *J. Am. Chem. Soc.* **120**, 2365 (1998).
6. A. L. Barra, A. Caneschi, A. Cornia, F. Fabrizi de Biani, D. Gatteschi, C. Sangregorio, D. R. Sessoli, and L. Sorace, *J. Am. Chem. Soc.* **121**, 5302 (1999).
7. A. L. Barra, A. Caneschi, D. Gatteschi, D. P. Goldberg, and R. Sessoli, *J. Solid State Chem.* **145**, 484 (1999).
8. J. Yoo, E. K. Brechin, A. Yamaguchi, M. Nakano, J. C. Huffman, A. L. Maniero, L.-C. Brunel, K. Awaga, H. Ishimoto, G. Christou, and D. N. Hendrickson, *Inorg. Chem.* **39**, 3615 (2000).
9. J. C. Goodwin, R. Sessoli, D. Gatteschi, W. Wernsdorfer, A. K. Powell, and S. L. Heath, *J. Chem. Soc. Dalton Trans.* 1835 (2000).
10. Early examples of metal-cyanide clusters, including some tetranuclear square clusters, can be found in Refs. (11–23).
11. R. F. Phillips and H. M. Powell, *Proc. R. Soc. Ser. A* **173**, 147 (1939).
12. J. J. Rupp and D. F. Shriver, *Inorg. Chem.* **6**, 755 (1967).
13. B. L. Shaw and G. Shaw, *J. Chem. Soc. (A)* 353 (1971).
14. F. Edelmann and U. Behrens, *J. Organomet. Chem.* **131**, 65 (1977).
15. W. C. Kalb, Z. Demidowicz, D. M. Speckman, C. Knobler, R. G. Teller, and M. F. Hawthorne, *Inorg. Chem.* **21**, 4027 (1982).
16. H. M. Dawes, M. B. Hursthouse, A. A. del Paggio, E. L. Muetterties, and A. W. Parkins, *Polyhedron* **4**, 379 (1985).
17. C. A. Bignozzi, S. Roffia, and F. Scandola, *J. Am. Chem. Soc.* **107**, 1644 (1985).
18. A. J. Deeming, G. P. Proud, H. M. Dawes, and M. B. Hursthouse, *Polyhedron* **7**, 651 (1988).
19. M. Zhou, B. W. Pfennig, J. Steiger, D. Van Engen, and A. B. Bocarsly, *Inorg. Chem.* **29**, 2456 (1990).
20. P. Braunstein, B. Oswald, A. Tiripicchio, and M. T. Camellini, *Angew. Chem. Int. Ed. Engl.* **29**, 1140 (1990).
21. M. Fritz, D. Rieger, E. Bär, G. Beck, J. Fuchs, G. Holzmann, and W. P. Fehlhammer, *Inorg. Chim. Acta* **198–200**, 513 (1992).
22. P. Schinnerling and U. Thewalt, *J. Organomet. Chem.* **431**, 41 (1992).
23. W. P. Fehlhammer and M. Fritz, *Chem. Rev.* **93**, 1243 (1993) and references therein.
24. W. R. Entley, C. R. Treadway, and G. S. Girolami, *Mol. Cryst. Liq. Cryst.* **273**, 153 (1995).
25. H. Weihe and H. U. Güdel, *Comments Inorg. Chem.* **22**, 75 (2000).
26. T. Mallah, S. Thiébaud, M. Verdaguer, and P. Veillet, *Science* **262**, 1554 (1993).
27. W. R. Entley and G. S. Girolami, *Science* **268**, 397 (1995).
28. S. Ferlay, T. Mallah, R. Ouahès, P. Veillet, and M. Verdaguer, *Nature* **378**, 701 (1995).
29. E. Dujardin, S. Ferlay, X. Phan, C. Desplanches, C. Cartier dit Moulin, P. Sainctavit, F. Baudelet, E. Dartyge, P. Veillet, and M. Verdaguer, *J. Am. Chem. Soc.* **120**, 11,347 (1998).

30. S. M. Holmes and G. S. Girolami, *J. Am. Chem. Soc.* **121**, 5593 (1999).
31. J. L. Heinrich, P. A. Berseth, and J. R. Long, *Chem. Commun.* 1231 (1998).
32. P. A. Berseth, J. J. Sokol, M. P. Shores, J. L. Heinrich, and J. R. Long, *J. Am. Chem. Soc.* **122**, 9655 (2000).
33. J. J. Sokol, M. P. Shores, and J. R. Long, *Angew. Chem. Int. Ed.* **40**, 236 (2001).
34. D. F. Shriver, S. A. Shriver, and S. E. Anderson, *Inorg. Chem.* **4**, 725 (1965).
35. K. R. Dunbar and R. A. Heintz, *Prog. Inorg. Chem.* **45**, 283 (1997) and references therein.
36. K. K. Klausmeyer, T. B. Rauchfuss, and S. R. Wilson, *Angew. Chem. Int. Ed.* **37**, 1694 (1998).
37. K. K. Klausmeyer, S. R. Wilson, and T. B. Rauchfuss, *J. Am. Chem. Soc.* **121**, 2705 (1999).
38. T. Mallah, C. Auburger, M. Verdaguer, and P. Veillet, *J. Chem. Soc. Chem. Commun.* 61 (1995).
39. A. Sculler, T. Mallah, M. Verdaguer, A. Nivorzhkin, J.-L. Tholence, and P. Veillet, *New J. Chem.* **20**, 1 (1996).
40. K. Van Langenberg, S. R. Batten, K. J. Berry, D. C. R. Hockless, B. Moubarak, and K. S. Murray, *Inorg. Chem.* **36**, 5006 (1997).
41. H. Oshio, O. Tamada, H. Onodera, T. Ito, T. Ikoma, and S. Tero-Kubota, *Inorg. Chem.* **38**, 5686 (1999).
42. Very recently, ground states of record high spin have been reported for pentadecanuclear metal-cyanide clusters (43, 44).
43. Z. J. Zhong, H. Seino, Y. Mizobe, M. Hidai, A. Fujishima, S. Ohkoshi, and K. Hashimoto, *J. Am. Chem. Soc.* **122**, 2952 (2000).
44. J. Larionova, M. Gross, M. Pilkington, H. Andres, H. Stoeckli-Evans, H. U. Güdel, and S. Decurtins, *Angew. Chem., Int. Ed.* **39**, 1605 (2000).
45. P. S. Bryan and J. C. Dabrowiak, *Inorg. Chem.* **14**, 296 (1975).
46. E. A. Schmitt, Ph.D. Thesis, University of Illinois at Urbana-Champaign (1995).
47. J. J. Borrás-Almenar, J. M. Clemente-Juan, E. Coronado, and B. S. Tsukerblat, *J. Comp. Chem.* **22**, 985 (2001).
48. M. Ohba, N. Usuki, N. Fukita, and H. Okawa, *Angew. Chem. Int. Ed.* **38**, 1795 (1999).
49. A. Marvilliers, S. Parsons, E. Rivière, J.-P. Audièrre, and T. Mallah, *Chem. Commun.* 2217 (1999).
50. W.-D. Griebler and D. Babel, *Z. Naturforsch. B* **37**, 832 (1982).
51. R. Eisenberg and J. A. Ibers, *J. Am. Chem. Soc.* **87**, 3776 (1965).
52. R. A. D. Wentworth, *Coord. Chem. Rev.* **9**, 171 (1972) and references therein.
53. P. M. Morse and G. S. Girolami, *J. Am. Chem. Soc.* **111**, 4114 (1989).
54. T. B. Karpishin, T. D. P. Stack, and K. N. Raymond, *J. Am. Chem. Soc.* **115**, 182 (1993).
55. P. B. Donaldson, P. A. Tasker, and N. W. Alcock, *J. Chem. Soc. Dalton Trans.* 1160 (1977).
56. K. Wieghardt, E. Schoffman, B. Nuber, and J. Weiss, *Inorg. Chem.* **25**, 4877 (1986).
57. A. A. Belal, I. Fallis, L. J. Farrugia, N. M. Macdonald, and R. D. Peacock, *J. Chem. Soc. Chem. Commun.* 402 (1991).
58. N. Arulsamy, J. Glerup, and D. J. Hodgson, *Inorg. Chem.* **33**, 3043 (1994).
59. M. B. Inoue, R. E. Navarro, M. Inoue, and Q. Fernando, *Inorg. Chem.* **34**, 6074 (1995).
60. M. Mikuriya, Y. Hatano, and E. Asato, *Bull. Chem. Soc. Jpn.* **70**, 2495 (1997).
61. E. I. Stiefel, R. Eisenberg, R. C. Rosenberg, and H. B. Gray, *J. Am. Chem. Soc.* **88**, 2956 (1966).
62. R. Hoffmann, J. M. Howell, and A. R. Rossi, *J. Am. Chem. Soc.* **98**, 2484 (1976).
63. D. L. Kepert, *Prog. Inorg. Chem.* **23**, 1 (1977).
64. S. K. Kang, T. A. Albright, and O. Eisenstein, *Inorg. Chem.* **28**, 1611 (1989).
65. A. Sculler, T. Mallah, M. Verdaguer, A. Nivorzhkin, J.-L. Tholence, and P. Veillet, *New J. Chem.* **20**, 1 (1996).
66. K. Kambe, *J. Phys. Soc. Jpn.* **5**, 48 (1950).
67. M. Verdaguer, T. Mallah, V. Gadet, I. Castro, C. Hélary, S. Thiébaud, and P. Veillet, *Conf. Coord. Chem.* **14**, 19 (1993).
68. S. Ohkoshi, O. Sato, T. Iyoda, A. Fujishima, and K. Hashimoto, *Inorg. Chem.* **36**, 268 (1997).
69. S. Ohkoshi and K. Hashimoto, *Chem. Phys. Lett.* **314**, 210 (1999).
70. J. C. Bonner and M. E. Fisher, *Phys. Rev. A* **135**, 640 (1964).
71. O. Kahn, "Molecular Magnetism," Chap. 11. VCH, New York, 1993.